

ABSTRACT / RESUMEN

Theoretical and numerical results are presented to assure that a tunable, narrow-band, coherent THz radiation source can be based on parametric down-conversion in a photonic crystal. Our proposal is based on down-conversion mixing and a local-field enhancement mechanism that is available by tuning each of the two driving laser fields either to band-edge or to a defect mode in the band gap. The frequency of the down-converted signal can be tuned by intersecting two non co-linear laser sources. The polarizations are degenerate at normal incidence and have sub-THz down-conversion maximum. For a specific sample geometry we show that by changing the angle of incidence of one tunable laser to 30 degrees the THz frequency is about 11.5 THz for p-polarization and 3.5 THz for s-polarization, since the angle-dependent transmission spectrum is different for p- and s-polarizations. The peak conversion efficiency for both polarizations is enhanced by over two orders of magnitude. Finally we also introduce some preliminary experimental results which agree with the numerical results we present here.

Terahertz Signal Generation in 1-D Photonic Crystals.

M. Torres-Cisneros*, J. W. Haus**, L. A. Aguilera-Cortés*, R. Guzmán-Cabrera*, R. Castro-Sánchez*, E. Alvarado-Méndez*, A. Andrade-Lucio*, R. Rojas-Laguna*, J. González-Barboza*, J. Estudillo-Ayala*, O. Ibarra-Manzano*, Mónica Trejo* and Angel González***.

INTRODUCTION

Optically driven sources that generate wavelengths corresponding to terahertz (THz) frequencies would be useful for an enormous number of imaging and sensing applications. Several techniques based on either novel schemes or exploiting well-known effects have been applied in order to develop THz sources. Each of these designs has different characteristics and works preferentially in a range of the wide THz region (0,1 THz-10 THz). The passive solid-state (Crowe, 1996) source design is one of the best proposals for the low frequency limits of the THz spectrum, although designs involve optical effects such as photoconductivity (PC) (Smith, 1988 and Benicewicz, 1993), optical parametric oscillation (Piestrup, 1975 and Minamide, 2001) (OPO), optical parametric generation (OPG) (Sato, 2002), optical rectification (Bass, 1962; Yang, 1971; Xu, 1992 and Chuang, 1992), photomixing (Aggarwal, 1974 and Brown, 1995)) and femtosecond pulse shaping (Weiner, 1990). Quantum cascade lasers (Tredicucci, 1998) form another branch of active THz device development. These sources can generate THz frequencies with output powers ranging from milliwatts to nanowatts.

Although new approaches to terahertz (THz) sources have been developed in the last two decades, potential applications in millimeter wave imaging, spectroscopy and others, have intensified the interest in developing a compact, intense, reliable and economic new THz source. From many different approaches to this problem, periodic media or photonic band gap (PBG) designs may be a viable and favorable option.

Periodic media have long been a topic of fascination for researchers. They form the basis of our understanding of a wide range of material properties. The mechanical and electrical properties of the materials can be explained by designing models

* FIMEE, University of Guanajuato. Av. Tampico 912, Salamanca, Guanajuato. 36730 Mexico. E-mail: mtorres@salamanca.ugto.mx.

** Electro-Optics Program, University of Dayton, Dayton, Ohio, 45469-0245 USA.

*** Universidad Politécnica de Puerto Rico, 377 Ave. Ponce de León, Hato Rey, 00918 San Juan PR.

KEYWORDS: Terahertz; Photonic Crystals; Sources.

PALABRAS CLAVE: Terahertz; Cristales Fotónicos; Fuentes.

En este trabajo presentamos resultados teóricos y numéricos que aseguran poder obtener una fuente de radiación coherente, sintonizable y de banda angosta en la región terahertz del espectro electromagnético. Nuestra propuesta se basa en el efecto de conversión paramétrica no lineal y en el mecanismo de amplificación del campo. Estos efectos se obtienen simultáneamente al sintonizar dos fuentes láser en la orilla de la banda prohibida o en el modo de un defecto localizado del cristal fotónico. La frecuencia de la señal obtenida puede ser sintonizada al mezclar las dos fuentes láser con diferente ángulo de incidencia. Las polarizaciones son degeneradas a un ángulo de incidencia normal y la conversión paramétrica genera señales sub-terahertz. Para una muestra específica, mostramos que cambiando el ángulo de incidencia de un láser sintonizable a 30 grados, la frecuencia de la señal obtenida en el cristal es de 11.5 THz para la polarización p y de 3.5 THz para la polarización s. Esto es debido a que el espectro de transmisión es dependiente del ángulo y por lo tanto, existen diferencias para la polarización p y para la s. La eficiencia de conversión pico para ambas polarizaciones es amplificada por más de dos órdenes de magnitud. Finalmente, también se muestran algunos resultados experimentales preliminares que concuerdan con los resultados numéricos que presentamos en este artículo.

Recibido: 23 de Marzo de 2004

Aceptado: 19 de Octubre de 2004

that elucidate the basic properties. These models necessarily lead to sets of coupled equations, whose analysis leads in a natural way to the concept of a Band structure. Band structure analysis is universally applicable to any system with periodic properties, whether the properties are described as essentially mechanical, electrical, optical, or quantum. These periodic systems universally give rise to responses which are periodic in time and space, i.e. waves. These waves can propagate with constant amplitude, or in the form of packets, or pulses. Waves traveling through these systems will travel at a speed which will be a function of their frequency, i.e. the systems will exhibit dispersion. Some frequencies will be allowed, while others may be forbidden, i.e. the system may have characteristics of a filter. The range of frequencies for which transmission is forbidden is said to constitute the "Band Gap" - the single most important property of such a system (Brillouin, 1953).

When light passes through a material, its electric field necessarily interacts with the atomic and molecular constituents of the material through the mechanism of polarization. Mathematically, this is described with dielectric tensors, for terms linear, quadratic, and higher order in the electric field. The linear dielectric constants are simply related to the indices of refraction - constants which are familiar to every student of physics. Thus, a periodic modulation of these optical constants will result in an optical system amenable to band structure analysis, and which may have a band gap. Hence, the term "Photonic Band Gap" (or "PBG") describes structures with such a property. These structures may be created with their periodicity extending over one, two, or three dimensions (Yariv, 1984 and Joannopoulos, 1995). The higher-dimensional systems present a special challenge to researchers; their fabrication, modeling, and analysis are complex. The formalism for calculating the system response (the transmission), as well as the band structure, of one dimensional PBG's has been well known for decades, and in the past they were typically referred to simply as "dielectric stacks", or "metal-dielectric stacks", as the case might be. The modern emphasis on the band-gap as the fundamental property of the structure, has provided a new vantage point, inspiring fresh research and new insights (Benedickson, 1996).

In terms of their technological applications, one dimensional PBG's are often introduced along with the physical concept of Bragg scattering. Bragg scattering occurs when the reflected or transmitted plane waves have their phase periodically modulated and recombine by constructive superposition to give an intense beam in a particular direction, for a particular wavelength or range of wavelengths (Yariv, 1984). Bragg scattering is often introduced to the student as a property associated with reflection, for example,

in the context of ruled mirror gratings. Such mirrors have a variety of applications, the best-known of which is their use as dispersive elements in spectrometers. However, Bragg scattering is also employed in technologically significant transmissive systems. For example, Bragg grating designs have recently proven useful in fiber optic systems, for performing a variety of multiplexing and filtering functions (Kashyap, 1999).

A light wave whose frequency lies within the band gap of a PBG, or whose frequency coincides with a transmission maximum or minimum, will also undergo Bragg scattering. Therefore, PBG's are significant to those technologies traditionally associated with Bragg scattering. However, PBG structures are also gaining attention as a promising approach to the implementation of a myriad of new technologies and applications. In 1987, Yablonovitch first proposed PBG's as a means of improving semiconductor laser efficiency and speed, by suppressing spontaneous emission (Yablonovitch, 1987). Since then, the applications of PBG structures have expanded greatly, along with the discovery of many of their important features (Joannopoulos, 1995 and Sakoda, 2002). For example, recent works have shown that one dimensional PBG's may be very promising for nonlinear frequency conversion (Centini, 1999 and Slusher, 2003).

Recently, Lu and co-workers (Lu, 2002) proposed the use of a nonlinear photonic crystal (also called a PBG) to generate coherent microwave radiation. They used the PBG characteristics in order to solve the velocity-matching problem. However, their analysis does not include an analysis of the important local field enhancement effects and dispersion due to finite-size effects. Therefore they do not predict the enhancement effects or the bandwidth limitations of the PBG THz sources.

In this work we propose to enhance the efficiency for parametric generation of THz radiation using PGB structures. Our approach

centers on either tuning the pump fields to a band-edge or a localized defect in the PBG structure. The physical phenomena involved in these THz regions are resonant field enhancement and increased density of electromagnetic states or equivalently the slow group velocity of the optical waves (Scalora, 1997). The combination of these effects can provide great flexibility in the design of new devices for THz or sub-THz wave generation.

RESULTS

We have explored several geometries using GaAs, as the first material, and materials, such as, AlAs, Al₂O₃ (alumina) or air, as the second material. Each one provides a larger index contrast. The final optimized structure does not rely on GaAs for the nonlinear mixing to generate THz radiation. Other materials such as, GaN or even organic polymers could be incorporated into final designs, based on the availability of fabrication techniques. In the following section we present two strategies for enhancing THz generation in PBGs: band-edge enhancement and defect-mode enhancement. From our studies we conclude that achieving two orders of magnitude enhancement of the signal probably has the greatest chance of success in a defect sample design.

Band-edge Enhancement

Sample geometry for band edge enhancement are shown in Figure 1; we consider a multi-layer sample with m periods. A GaAs substrate is shown, but we also explore the case of an air substrate for comparison. The number of periods is changed to determine the enhancement effects. The enhancement grows as the number of layers is increased; however, the bandwidth of the resonance also decreases as more layers are added.

In Figures 2 the transmission spectra for the same GaAs/AlAs multi-layer stack is shown. The figure 2a has an air substrate and figure 2b has a GaAs substrate. The layer thicknesses are

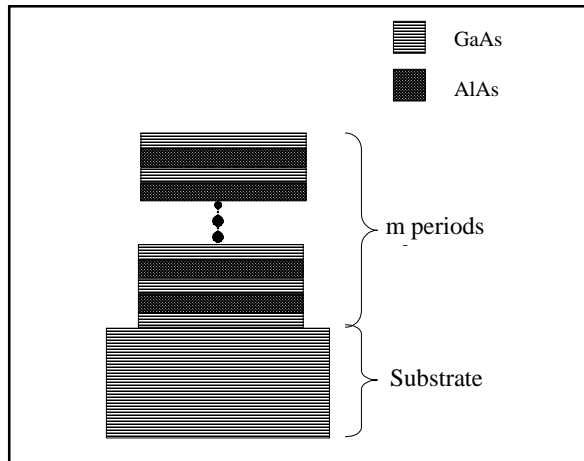


Figure 1. Sample geometry: GaAs/AlAs layers with a GaAs substrate. The box with lines denotes GaAs and the box with dots denotes one of the other materials, such as AlAs.

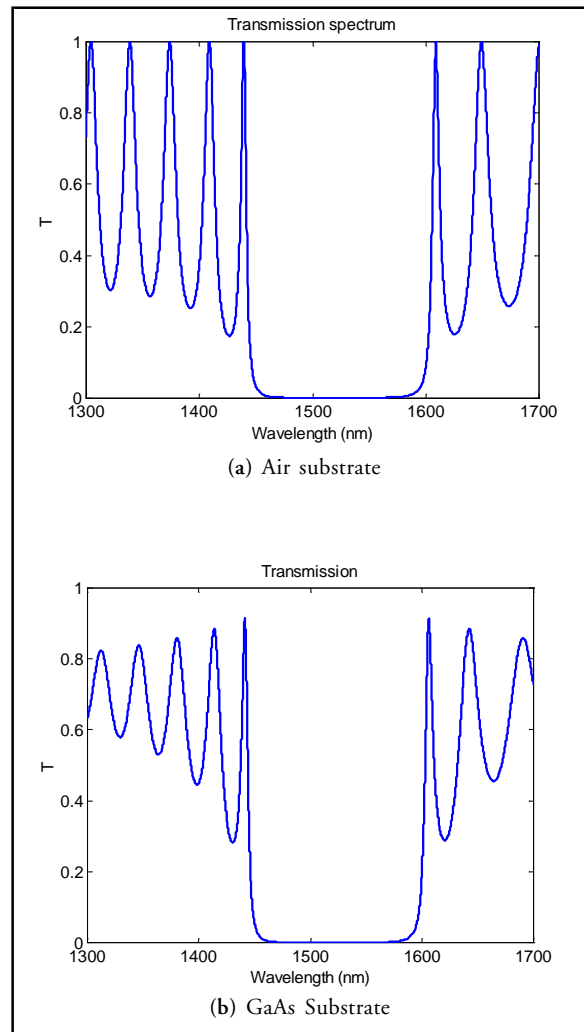


Figure 2. Transmission spectrum for 30 periods GaAs/AlAs. Air substrate (a) and infinite GaAs substrate (b).

$d(\text{GaAs})=112,51 \text{ nm}$ and $d(\text{AlAs})=130,45 \text{ nm}$. The PBG stack has 30 periods. The first transmission resonance at the long wavelength side of the band gap has a resonant field as shown in Figures 3. Figure 3a shown the field intensity for air substrate and Figure 3b for GaAs substrate. The GaAs substrate overall has smaller field values. The input and output field intensity is nearly unity for the air substrate. In both cases the envelope of the field has a single maximum.

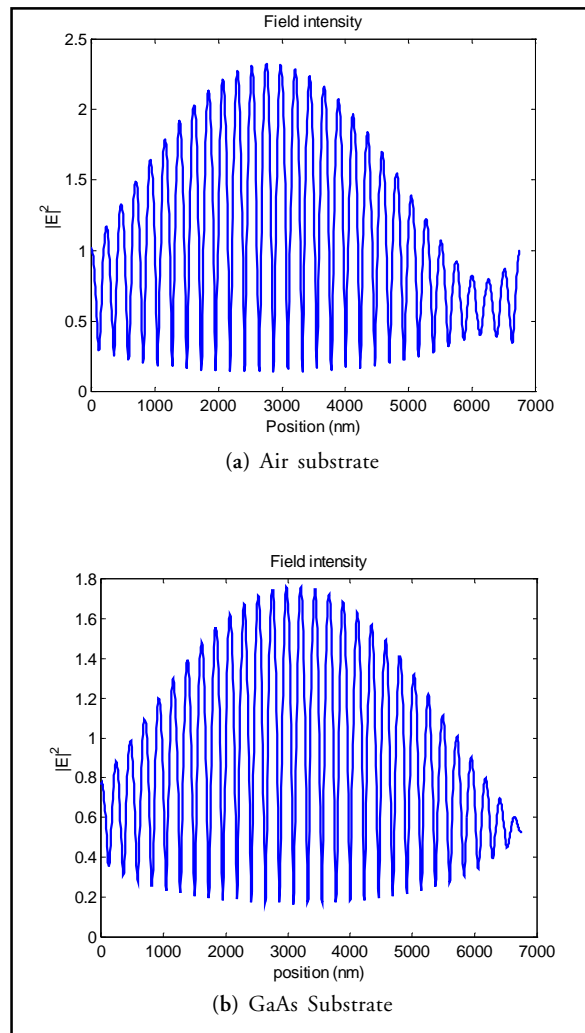


Figure 3. Envelope of the field for a 30 period multi-layer stack. (a) Has an air substrate and (b) has a GaAs substrate. The field is shown for the first transmission maximum, which occurs at the wavelength, $\lambda=1608.7 \text{ nm}$ (a), and $\lambda=1606.2 \text{ nm}$ (b). Note the vertical axis should be $|E|$ and not its square.

By taking the product of two fields at different wavelengths and integrating over the sample we determine the THz signal enhancement. The normalization is the expected THz signal when the sample is perfectly phase matched in a homogeneous sample. This is a crude measure that assumes the second-order nonlinearity is homogeneous. Our samples are much smaller than the wavelength and therefore propagation effects are negligible.

$$I = \left| \int_0^L E_1 E_2^* dz \right|^2 / L^2 \quad (1)$$

where E_i represents the complex electric field and L is the length of the sample.

The enhancement in the 30-period GaAs/AlAs with Ga As substrate case is only of order unity, as shown in Figure 4b but it increase about 60 % for Air substrate case, Figure 4a. The bandwidth of the resonance is about 1 THz. Increasing the number of layers increases the enhancement. Figures 5 and 6 illustrate the field profile and the band-edge enhancement for 60 and 100 periods. The (a's) Figures show the transmission band and the (b's) Figures show the electric field enhancement at the long wavelength band edge. Note that as the peak enhancement increases, the bandwidth decreases.

Our initial numerical analysis uses two laser beams at normal incidence on a 1D photonic crystal. The sample is composed of a multi-

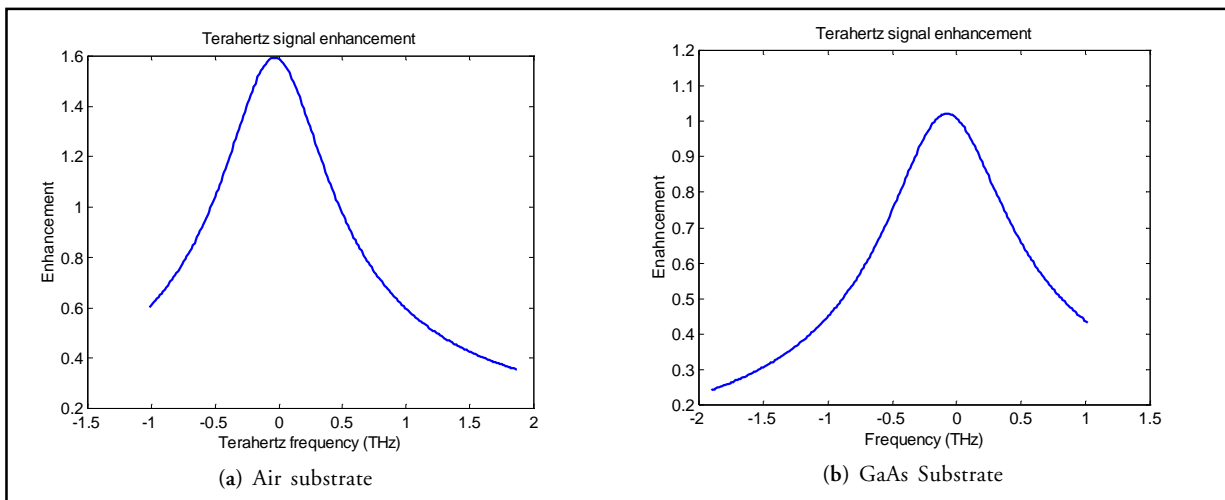


Figure 4. Enhancement of the THz signal for the 30 period samples as discussed above. (a) Has an air substrate and (b) has a GaAs substrate.

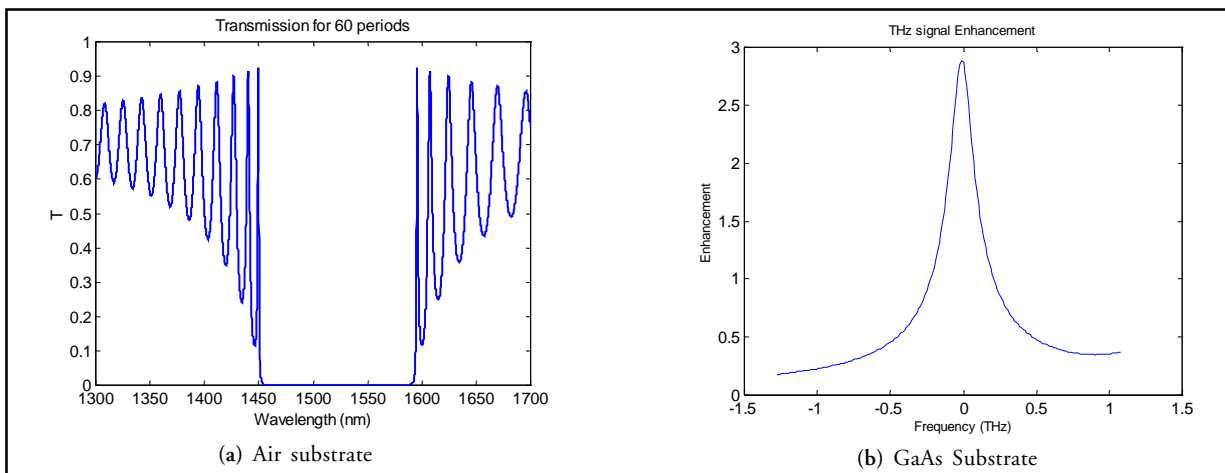


Figure 5. (a) Transmission spectrum and (b) enhancement for a 60 period GaAs/AlAs sample with GaAs substrate.

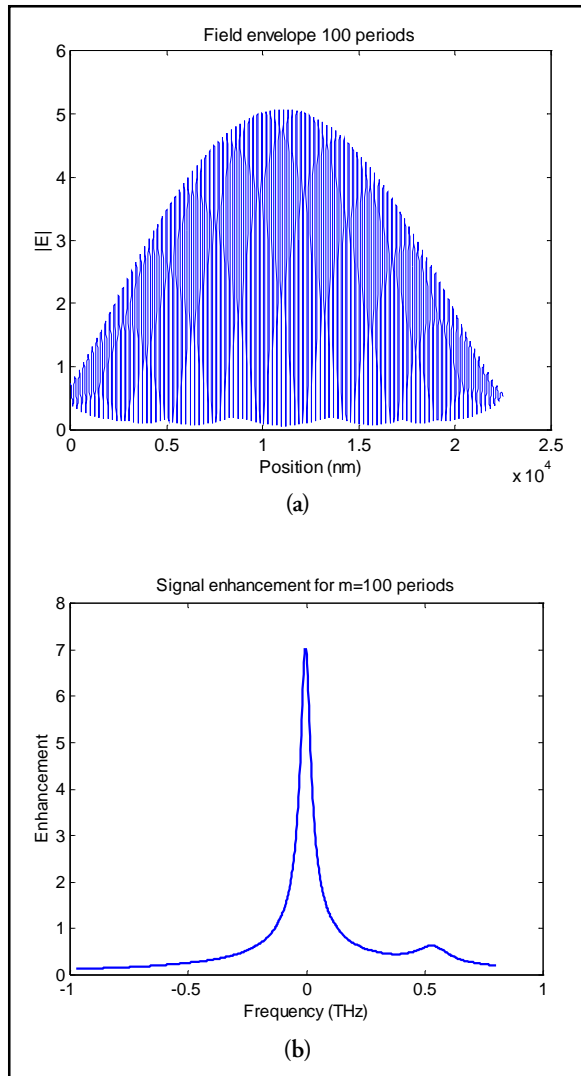


Figure 6. (a) Field envelope and (b) enhancement for a 100 period sample of GaAs/AlAs with GaAs substrate.

layer array with m periods deposited on a substrate. One period in the array consists of one layer of GaAs and one layer of other of Al_2O_3 , both a quarter-wave thick. A GaAs substrate was studied, but we also explored an air interface on each side for comparison. Two detuned laser fields were used to generate the THz signal. The first laser field was tuned at a wavelength, which coincided with the first transmission resonance (around 1 330 nm). The second laser field wavelength was varied around the first one in order to calculate the enhancement and the bandwidth. The layer thicknesses were fixed at $d(\text{GaAs}) = 71,42$ nm and $d(\text{Al}_2\text{O}_3) = 166,66$ nm.

A comparison of the transmission spectra for the same GaAs/ Al_2O_3 multi-layer stack changing the substrate shows that the large refraction index contrast for the air-substrate case, generates higher transmission peaks. The fields located at the first transmission resonance at the edge of the band gap revealed that the GaAs-substrate has smaller resonant-field values in the PBG. We determine the THz signal enhancement by taking the products of two fields in the sample, located at different wavelengths, integrating over the sample and normalizing with respect to the nonlinear length. The number of periods in the sample is changed to determine the enhancement effects. The enhancement grows as the number of layers is increased; as previously mentioned the bandwidth of the resonance also decreases as more layers are added.

Figure 7 shows the THz enhancement obtained for two different samples that differ in the numbers of layer pairs. The enhancement is compared against the result expected for a homogeneous GaAs material of the sample thickness. Our samples are very thin compared to the THz wavelength. For 40 layers the THz signal enhancement is about 35; increasing the number of layers by 33 % results in a about a factor of four increase in the peak signal enhancement. The bandwidth of the enhancement decreases at the same time. The behavior of the THz enhancement and the bandwidth versus the number of layers is shown

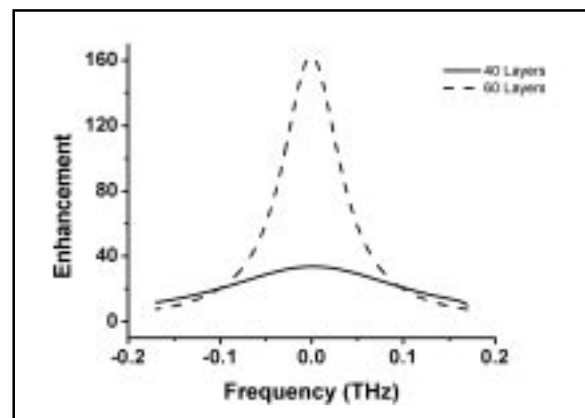


Figure 7. THz signal enhancement versus number of layers.

in Figure 8. Here we observe the enhancement is achieved at the cost of bandwidth. For about 60 layers the bandwidth is around 100 GHz reduced from a value around 400 GHz for 40 layers.

Angle tuning

The frequency of the down-converted signal can be tuned by intersecting two non co-linear laser sources. Suppose that one laser is normally incident on the medium and the second laser is non-normally incidence, which shifts the transmission maximum and the band edge. The same parameters are used here as for the dashed curve in Figure 8 ($N = 60$, $d(\text{GaAs}) = 71,42 \text{ nm}$, $d(\text{Al}_2\text{O}_3) = 166,66 \text{ nm}$). At non-normal incident angles the transmission spectrum is different for p- and s-polarizations. We find that the p-polarization has a much larger shift than the s-polarization for the same angle of incidence. Figure 9 displays the transmittance for normal incidence and the p- and s-polarizations incident at 15 degrees from the normal. The widths of both resonances do not appreciably change and the field enhancement inside the PBG structures is similar for both cases.

Figures 10a and b show that the overlap of the two fields is excellent and the enhancement is 150 and 180 for p- and s-polarizations, respectively. The p-polarization has a maximum

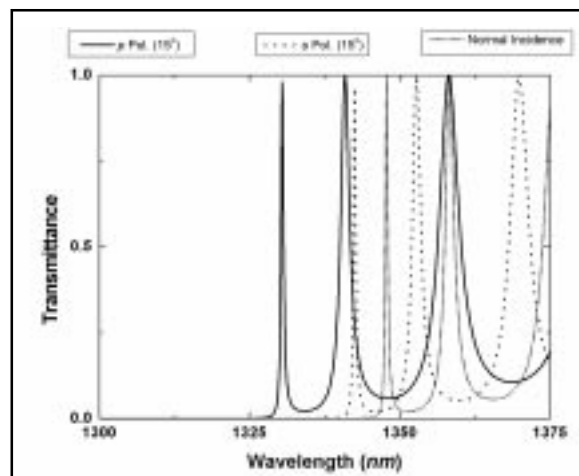


Figure 9. Transmission spectra for normal incidence and 15 degree angle of incidence. The p- and s-polarizations have different shifts of their band-edge resonance peaks, but the resonance width is nearly the same.

enhancement frequency at 5,15 THz, while for s-polarization the maximum is at 1,55 THz. Figure 11 highlights our results on the dependence of the THz emission with the angle tuning of the THz emission. The polarizations are degenerate at normal incidence and have their maximum near zero frequency. By tuning out to 30 degrees the signal frequency at the maximum enhancement is about 11,5 THz for p-polarization and 3,5 THz for s-polarization. The peak enhancement for both polarizations remains over two orders of magnitude. The bandwidth of the enhancement peaks remains around 75 GHz over the entire range of angles.

Defect Enhancement

A second mechanism for THz enhancement is the use of a localized defect mode in a photonic crystal. Typically a quarter-wave crystal sandwiches a layer that is some multiple of a half-wave layer thickness. In our planned experiments using a OPG/OPA source the bandwidth of the source laser pulses is about 3 GHz, which is small enough for our experimental design. The sample, labeled MB 3 027, was obtained for initial experiments. We use the design parameters of that sample for our demonstration of defect-mode local field enhancement. The sample geometry is shown in Figure 12.

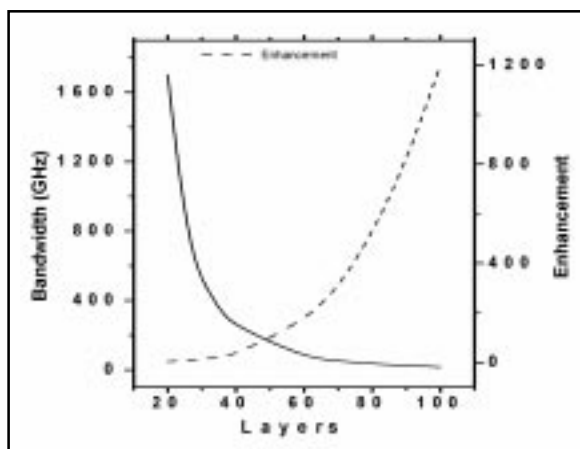


Figura 8. Down-conversion signal enhancement and bandwidth versus the number of layer pairs for GaAs/Al₂O₃ PBGs. The parameters are the same as in Fig. 5.

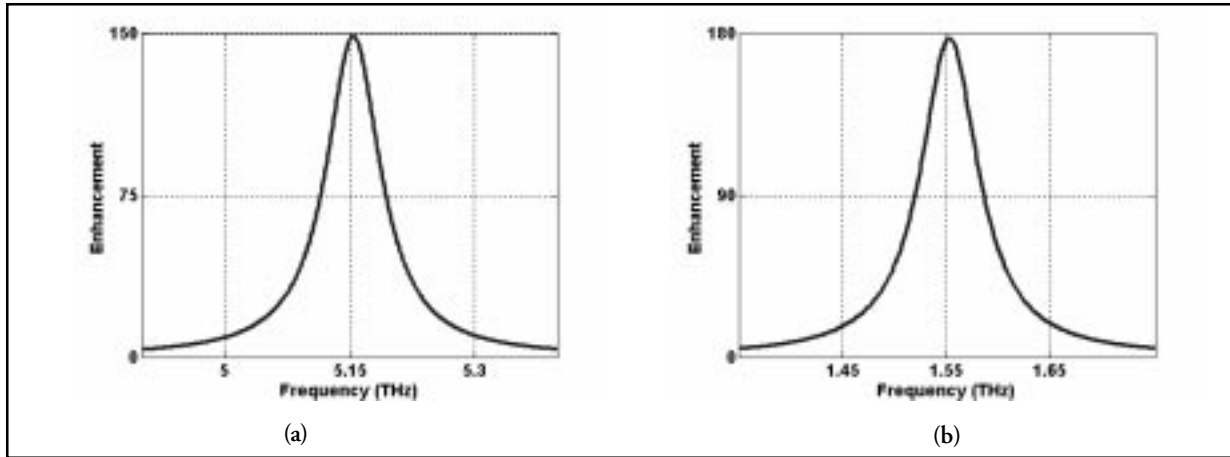


Figure 10. Resonance enhancement of the THz signal for (a) p-polarization and (b) s-polarization. The peak is shifted into the THz regime and the resonance width remains narrow.

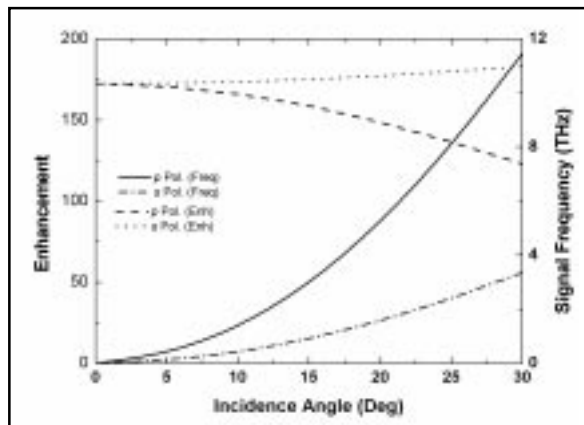


Figure 11. Enhancement and Signal frequency versus angle of incidence for p- and s-polarizations.

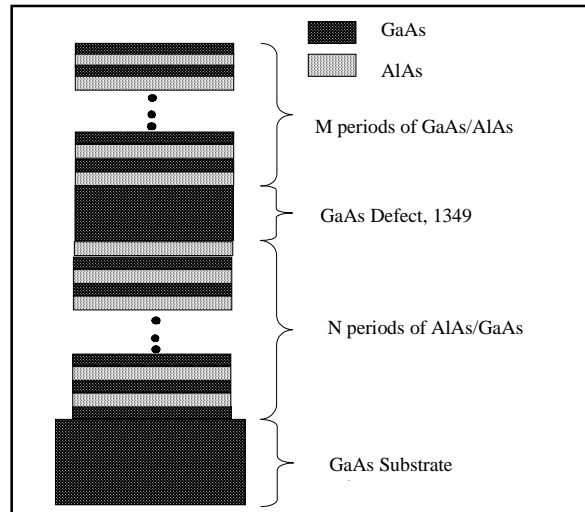


Figure 12. Experimental sample geometry. The defect creates an enhanced field that extends over the entire sample. The dotted box denotes GaAs and the cross-hatched box denotes AlAs. Sample geometry: Air/GaAs/AlAs/Defect(GaAs)/AlAs/GaAl/Substrate(GaAs). 18 periods/defect/22periods/substrate. Thickness: $d_1=112,42$ nm(GaAs), $d_2=130,45$ nm (AlAs), $d_3=1\ 349$ nm (GaAs defect).

The calculated transmission spectrum for the sample is shown in Figure 13 in the regime from 1 400 nm-1 700 nm; a defect-mode is present in the center of the gap. The transmission curve is very sharp at the defect-mode position, which is peaks at 1 518,87 nm; plotting points were chosen on a grid with 0,05 nm spacing; near the defect the plotting points are separated by 0,01 nm. The defect mode in the center is sharp and is indicates a large Q-factor for that mode. The field when the wavelength is tuned to the maximum transmission at the defect is shown in Figure 14. The resonant intensity is increased by two orders of magnitude.

At normal incidence the magnitude of the enhancement for this case is about 550. It represents almost three orders of magnitude enhancement over the band-edge enhancement case shown in Figure 4. The resonant width of the enhancement peak is about 40 GHz, which is wide enough to minimize the laser bandwidth effects. However, by angle tuning one laser we

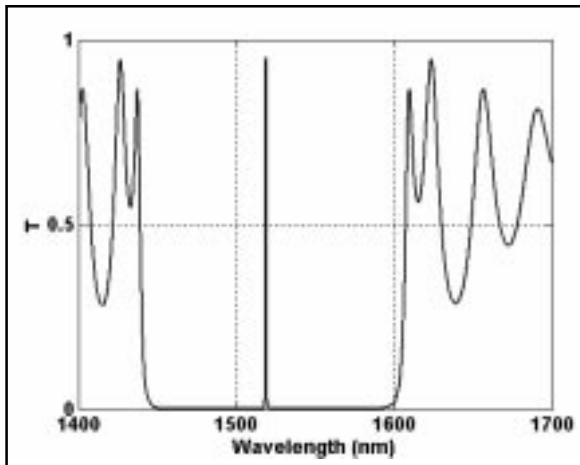


Figure 13. Transmission spectra for GaAs/AlAs sample with defect mode shown in the band gap.

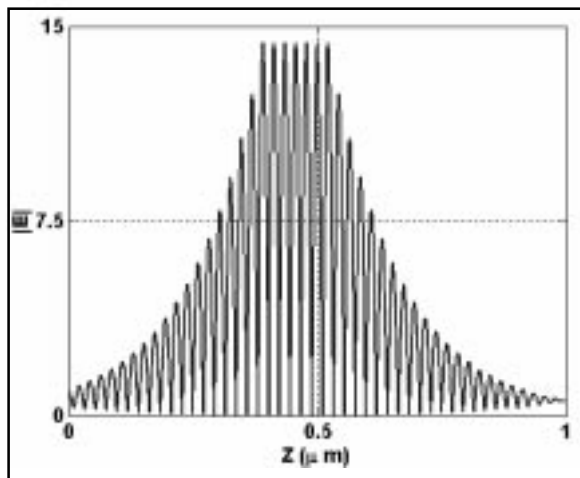


Figure 14. Field profile at the maximum transmission of the defect mode.

again observe a shift of the resonance position for both polarizations. The enhancement versus tuning frequency for 30 degrees angle of incidence is shown in Figure 15. The shift is much smaller for our defect example than it was for the band-edge cases discussed in the previous section. At 30 degrees angle of incidence, the peak enhancement occurs at 2,3 THz, but the size of the enhancement, about 420 for the p-polarization, remains large over the entire range of angles. The s-polarization shift is identical to the p-polarization shift in this case and we do not separately plot that result. The bandwidth remains very narrow. By

using larger angles of incidence the frequency can be shifted to greater values, but remains well below 10 THz out to angles of incidence of 80 degrees.

Transmission through the experimental crystal (MB 3027)

Initial experiments will be performed using a sample (named MB 3027) that became available, but was designed for a different application. The experimental transmission through the sample MB 3027 was measured using two techniques. The first was a IR spectrophotometer. The transmission spectrum was measured with 1 nm and 0,5 nm resolution. There is no distinguishable difference between the two measurements, except at the defect position, Figure 16. In the 1 nm resolution the peak was only a few percent. However, for the 0,5 nm case the peak increased to about 13 %. Using a tunable diode laser further increased the defect-mode transmission to about 36 % (Figure 17).

The measured wavelength of the defect-mode is within 1 nm of the calculated wavelength. The parameters were used based on the growth parameters quoted from the foundry and the index parameters from the literature. The agreement between theory and experiment

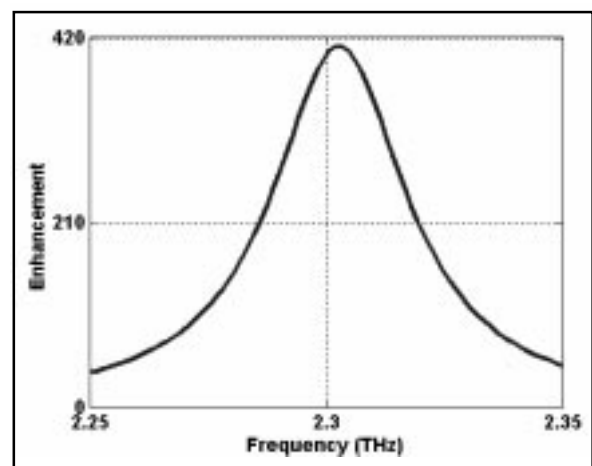


Figure 15. Enhancement of the signal versus frequency. The angle of incidence of the second laser is 30 degrees. Only p-polarization is shown here.

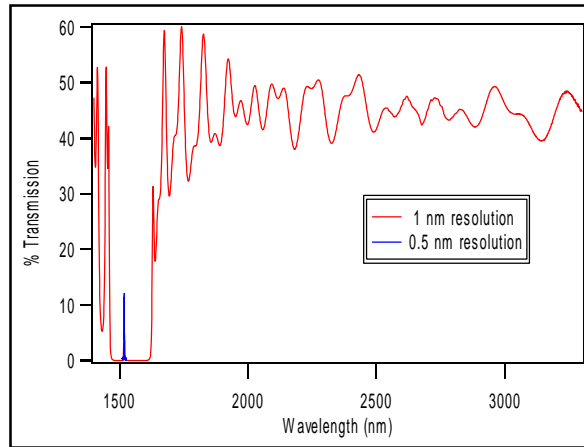


Figure 16. Transmission through PBG sample using 1 nm resolution. The smaller scan was done at 0.5 nm resolution. The measurement was made using a Cary 5000 spectrophotometer.

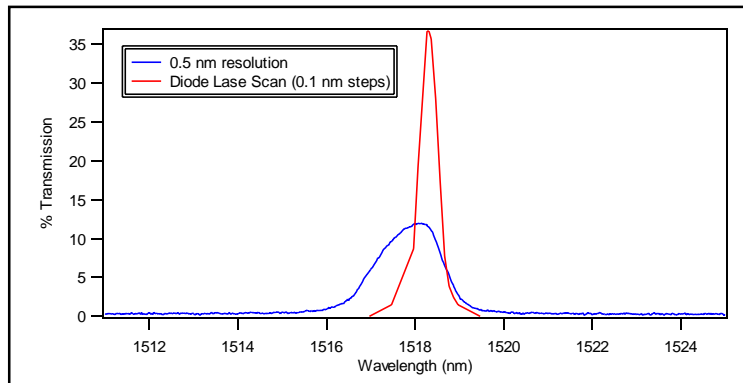


Figure 17. Measurement of the defect mode with spectrophotometer and diode laser. Defect-mode transmission curves with the photospectrometer have 0.5 nm resolution. The diode laser was stepped through the spectral region of the defect 0.1 nm at a time.

forms a good calibration for future experiments to measure the THz emission from the sample. An experimental test of our enhancement concept is planned in the near future. An experiment using a tunable OPG and OPA source will meet the design criteria. We are obtaining a bolometer for the THz measurements.

CONCLUSIONS

In this paper we reported the local-field enhancement effect to efficient THz generation using either a defect-mode or a band-edge tuning position. Two lasers are mixed at

precisely detuned wavelengths and the sources are tuned to the resonance feature by adjusting the angle of incidence. For a defect-mode geometry we demonstrated that by changing the angle of incidence of one tunable laser to 30 degrees the THz frequency is tuned over a range of about 11,5 THz for p-polarization and 3,5 THz for s-polarization, since the angle-dependent transmission spectrum is different for p- and s-polarizations. The peak conversion efficiency for both polarizations is enhanced by over two orders of magnitude.

The bandwidth of the enhancement peaks remains around 75 GHz over the entire range of angles. A localized defect mode can also be exploited as a mechanism to enhance THz signals in a PBG. It represents almost three orders of magnitude enhancement over the band-edge enhancement case. However, by using the angle tuning of one laser we found that the shift is much smaller for our defect sample than it was for the band-edge case. We also estimated that the magnitude of the THz signal would be about 10 μ W for a 1 W laser input power due to the low quantum efficiency of the down-conversion process.

ACKNOWLEDGEMENTS

This work was partially supported by a DARPA grant, the NSF grant ECS-0140109, an University of Guanajuato grant through the program "Programa Institucional de Fortalecimiento a la Investigación 2003" and CONCYTEG-5987-FONINV, through the project "Apoyo a la maestría en Ing. Eléctrica". The authors would like to dedicate this work to the memory of asterisC^o.

REFERENCES

- Aggarwal R. L., Lax B., Fetterman H.R., Tannenwald P. E., Clifton B. J. (1974). CW generation of tunable narrow-band far-infrared radiation. *Journal of Applied Physics*, 45: 3972-3974.

- Bass M., Franken P. A., Ward J. F., Weinreich G. (1962). Optical Rectification. *Physics Review Letters*, 9: 446-448.
- Benedickson J. M., Dowling J. P. and Scalora M. (1996). Analytic expressions for the electromagnetic mode density in finite, one-dimensional, photonic band-gap structures. *Physical Review B*, 53: 4107-412.
- Benicewicz P. K., Taylor A. J. (1993). Scaling of terahertz radiation from large-aperture biased InP photoconductors. *Optics Letters*, 18: 1332-1334.
- Brillouin L. (1953). Wave propagation in periodic structures. *Dover*, NY.
- Brown E. R., McIntosh K. A., Nichols K. B., and Dennis C. L. (1995). Photomixing up to 3.8 THz in low temperature-grown GaAs. *Applied Physics Letters*. 66: 285.
- Centini M., Sibilia C., Scalora M., D'Aguanno G., Bertolotti M., Bloemer M. J., Bowden, C.M., Nefedov I. (1999). Dispersive properties of finite, one-dimensional photonic band gap structures: Applications to nonlinear quadratic interactions. *Physical Review E*. 60: 4891-4898.
- Chuang S. L. (1992). Optical rectification at semiconductor surfaces. *Physical Review Letters*. 68: 102-105.
- Crowe T. W., Grein T. C., Zimmermann R. , and Zimmermann P. (1996). Progress toward solid-state local oscillators at 1 THz. *IEEE Microwave Guided Wave Letters*. 6: 207-208.
- Haus J. W., Powers P., Bojja P., Torres-Cisneros M., Scalora M., Bloemer M., Akozbek N. and Meneses-Nava M. (2004). Enhanced Tunable Terahertz generation in photonic band gap structures. *Laser Physics*. 14: 5.
- Joannopoulos J. D., Meade R. D. and Winn J. N. (1995). Photonic Crystals. *Princeton University Press*. NJ.
- Kashyap R. (1999). Fiber Bragg Gratings, *Academic*. Boston.
- Lu Yan-qing, Xiao Min, Salamo Gregory J. (2002). Coherent microwave generation in nonlinear photonic crystal. *IEEE Journal of Quantum Electronics*. 38: 481-485.
- Minamide H., Kawase K, Imai K., Sato A., Ito H. (2001). A continuously tunable ring-cavity THz-wave parametric oscillator. *Review of Laser Engineering*. 29: 744-748.
- Piestrup M.A., Fleming R.N. (1975). Continuously tunable sub-millimeter wave source. *Applied Physics Letters*. 26: 418-419.
- Sakoda K. (2002). Optical Properties of Photonic Crystals. *Springer*. Berlin.
- Sato A., Imai K., Kawase K., Minamide H., Wada S., Ito H. (2002). Narrow-linewidth operation of a compact THz-wave parametric generator system. *Optics Communications*. 207: 353-359.
- Scalora M., Bloemer M.J., Manka A.S., Dowling J.P., Bowden C.M., Viswanathan R., Haus J.W. (1997). Pulse second-harmonic generation in nonlinear, one-dimensional, periodic structures. *Physics Review A*. 56: 3166-3174.
- Slusher R. E. and Eggleton B. J. Eds., (2003). Nonlinear Photonic Crystals. *Springer Series in Photonics, Volume 10*. Berlin.
- Smith P. R., Auston D. H. and Nuss M. C. (1988). Subpicosecond photoconducting dipole antennas. *Journal of Quantum Electronics*. 24: 255-260.
- Tredicucci A., Capasso F., Gmachl C., Sivco D.L., Hutchinson A.L., Chao A.Y. (1998). High performance interminiband quantum cascade lasers with grades superlattices. *Applied Physics Letter*. 73: 2101-2103.
- Weiner A. M. and Leaird D. E. (1990). Generation of terahertz-rate trains of femtosecond pulses by phase only filtering. *Optics Letters*, 15: 51-53.
- Xu L. Zhang X. C. and Auston D. H. (1992). Terahertz beam generation by femtosecond optical pulses in electro-optic materials. *Applied Physics Letters*. 61: 1784-1786.
- Yablonovitch E. (1987). Inhibited spontaneous emission in solid-state physics and electronics. *Physics Review Letters*. 58: 2059-2062
- Yang K. H., Richards P. L., Shen Y. R. (1971). Generation of far-infrared radiation by picosecond light pulses in LiNbO₃. *Applied Physics Letters*. 19: 320-323.
- Yariv A. and Yeh P. (1984). *Optical Waves in Crystals*. Wiley-Interscience. New-York.